

# New multicomponent forms of the antiretroviral Nevirapine with improved dissolution performance

*Rogeria N. Costa,<sup>†\*</sup> Ana L. Reviglio,<sup>§,¥</sup> Sana Siedler,<sup>‡</sup> Simone G. Cardoso,<sup>‡</sup> Yamila*

*G. Linck,<sup>§,¥</sup> Gustavo A. Monti,<sup>§,¥</sup> Alexandre M. G. Carvalho,<sup>¶</sup> Jackson A. L. C.*

*Resende,<sup>††</sup> Marcelo H. C. Chaves,<sup>‡‡</sup> Helvécio V. A. Rocha,<sup>‡‡</sup> Duane Choquesillo-*

*Lazarte,<sup>§§</sup> Lourdes Infantes,<sup>¶¶</sup> Silvia L. Cuffini<sup>†\*</sup>*

<sup>†</sup>Instituto de Ciência e Tecnologia (ICT), Universidade Federal de São Paulo

(UNIFESP), 12231-280 São José dos Campos, Brazil. <sup>§</sup>FaMAF-Universidad

Nacional de Córdoba, 5016 Córdoba, Argentina. <sup>¥</sup>IFEG-CONICET, 5016 Córdoba,

Argentina. <sup>‡</sup>Centro de Ciências da Saúde (CCS), Universidade Federal de Santa

Catarina (UFSC), 88040-900 Florianópolis, Brazil. <sup>¶</sup>Laboratório Nacional de Luz

Síncrotron (LNLS), Centro Nacional de Pesquisa em Energia e Materiais

(CNPEM), 13083-100 Campinas, Brazil. <sup>††</sup>Universidade Federal Fluminense

(UFF), 24020-150 Niterói, Brazil. <sup>‡‡</sup>Laboratório de Micro e Nanotecnologia (LMN),

Farmanguinhos, Fundação Oswaldo Cruz (FIOCRUZ), 21040-361 Rio de Janeiro,

Brazil. <sup>§§</sup>Laboratorio de Estudios Cristalográficos, IACT (CSIC-UGR), Avda. de las

Palmeras 4, 18100 Armilla, Granada, Spain. <sup>¶¶</sup>Instituto de Química Física

Rocasolano (IQFR), Consejo Superior de Investigaciones Científicas (CSIC),

28006 Madrid, Spain.

## Supplementary Material

### *Sample preparation – experimental details:*

NVP raw material was manufactured by Nortec Química. Seven co-formers were tested: salicylic acid (SA), 3-hydroxybenzoic acid (3HBZC), 4-hydroxybenzoic acid (4HBZC), saccharin (SAC), caffeine (CAF), theophylline (THEO), and urea (URE).

All the multi-component forms of NVP were prepared through the liquid-assisted grinding (LAG) method. The NVP and the co-former were placed in stainless steel grinding jar with 3 drops of solvent. Methanol and chloroform were tested as solvents in different sample preparations. NVP and co-former were ground at stoichiometric ratios 1:1 and 2:1. Stainless steel balls with 5 mm in diameter were added to the tube which was placed in a roller mill system. The mixture was ground for 24 hours. Subsequently, materials were dried at 40 °C for 48 hours to generate powder samples. Single crystals were obtained through saturation in chloroform followed by slow solvent evaporation. All reagents and solvents were at an analytical grade.

*Preparation of files for calculations:*

The files used in the molecular complementarity (MC) and H-bond propensity (HBP) calculations were previously prepared. In MC, mol2 files of NVP and all co-formers were necessary. These files were obtained from structures already deposited on the CSD database and are mentioned below (Table S1). In those cases where more than one molecule was present in the structure, these exceed molecules were manually deleted and the file was saved containing just one molecule. All process was performed through CCDC Mercury software v.4.0.0.

In addition, for HBP files containing both NVP and co-former molecules together were prepared. This was necessary to assess the probability for all possible donors and acceptors for both molecules simultaneously.

Table S1. CSD refcode used in MC and HBP calculations for NVP and the co-formers.

<b>Coformer</b>	<b>CSD refcode</b>
<i>Nevirapine</i>	<b>PABHIJ</b>
<i>Salicylic acid</i>	<b>SALIAC</b> <b>SALIAC03</b>
<i>3-Hydroxybenzoic acid</i>	<b>BIDLOP02</b>
<i>4-Hydroxybenzoic acid</i>	<b>JOZZIH01</b>
<i>Saccharin</i>	<b>SCCHRN</b>
<i>Caffeine</i>	<b>NIWFEE03</b>
<i>Theophylline</i>	<b>BAPLOT01</b>
<i>Urea</i>	<b>UREAXX</b>

Table S2. Molecular complementarity (MC) results for Nevirapine and the selected co-formers.

			M/L axis ratio	S axis (Å)	S/L axis ratio	dipole moment magnitude	fraction of Nitrogen and Oxygen	
Nevirapine	PABHLJ		0,895	6,667	0,611	1,972	0,25	

Cofomer	Refcode	Overall PASS/FAIL	M/L axis ratio	M/L axis ratio Delta  (pass < 0.31)	M/L axis ratio pass/fail	S axis (Å)	S axis (Å) Delta  (pass < 3.23)	S axis (Å) pass/fail	S/L axis ratio	S/L axis ratio Delta  (pass < 0.275)	S/L axis ratio pass/fail	dipole moment magnitude (Debye)	dipole moment magnitude (Debye) Delta  (pass < 5.94)	dipole moment magnitude (Debye) pass/fail	fraction of N and O	fraction of N and O Delta  (pass < 0.294)	fraction of N and O pass/fail
Salicylic acid	SALIAC	FAIL	0,788	0,106	pass	3,418	3,249	fail	0,368	0,243	pass	1,693	0,279	pass	0,300	0,050	pass
Salicylic acid	SALIAC03	PASS	0,789	0,106	pass	3,449	3,218	pass	0,372	0,239	pass	1,622	0,349	pass	0,300	0,050	pass
3-Hydroxybenzoic acid	BIDLOP02	PASS	0,815	0,079	pass	3,470	3,197	pass	0,373	0,238	pass	1,428	0,544	pass	0,300	0,050	pass
4-Hydroxybenzoic acid	JOZZIH01	PASS	0,673	0,221	pass	3,460	3,207	pass	0,347	0,263	pass	2,078	0,106	pass	0,300	0,050	pass
Saccharin	SCCHRN	PASS	0,954	0,059	pass	5,480	1,187	pass	0,620	0,009	pass	2,109	0,137	pass	0,333	0,083	pass
Caffeine	NIWFEE03	PASS	0,864	0,030	pass	4,261	2,406	pass	0,423	0,187	pass	1,123	0,849	pass	0,429	0,179	pass
Theophylline	BAPLOT01	PASS	0,877	0,017	pass	4,271	2,396	pass	0,427	0,183	pass	0,836	1,136	pass	0,462	0,212	pass
Urea	UREAXX	FAIL	0,880	0,015	pass	3,400	3,267	fail	0,526	0,084	pass	1,539	0,433	pass	0,750	0,500	fail

*PXRD results:*

Figure S1 exhibits the powder diffraction results for pure compounds and NVP-3HBZC, NVP-4HBZC, NVP-THEO, NVP-CAF, and NVP-URE samples. Samples were prepared through the LAG method, using chloroform and 1:1 stoichiometry. PXRD results indicate the formation of NVP-3HBZC and NVP-4HBZC cocrystals. The diffraction pattern for NVP-4HBZC exhibits just a single crystalline phase, whereas the diffraction pattern for NVP-3HBZC exhibits a mixture of a new phase and a phase corresponding to 3HBZC. On the other hand, PXRD results for NVP-THEO, NVP-CAF, and NVP-URE indicate a mixture of crystalline phases corresponding to NVP and co-former.

As we have described before, in the present work, we have prepared NVP-SA and NVP-SAC cocrystals through the LAG method, using chloroform or methanol in the preparations and with 1:1 and 2:1 stoichiometries. Caira and co-workers<sup>1</sup> have obtained and described both NVP-Salicylic acid and NVP-Saccharin cocrystals. They have obtained NVP-Salicylic acid cocrystal through the solvent-

drop method, using 1:1 stoichiometry and methanol. The structure they have deposited presents 2 to 1 stoichiometry for NVP and SA respectively. In addition, the NVP-saccharin single crystal was obtained through a slow-evaporation method using 1:1 stoichiometry in methanol solvent. Although other experiments were conducted in that work, they have not described the preparation through the LAG method using methanol. Moreover, Caira et al.<sup>1</sup> have described the preparation of NVP-Saccharin through LAG using chloroform and 1:1 stoichiometry, resulting in a 2:1 cocrystal.



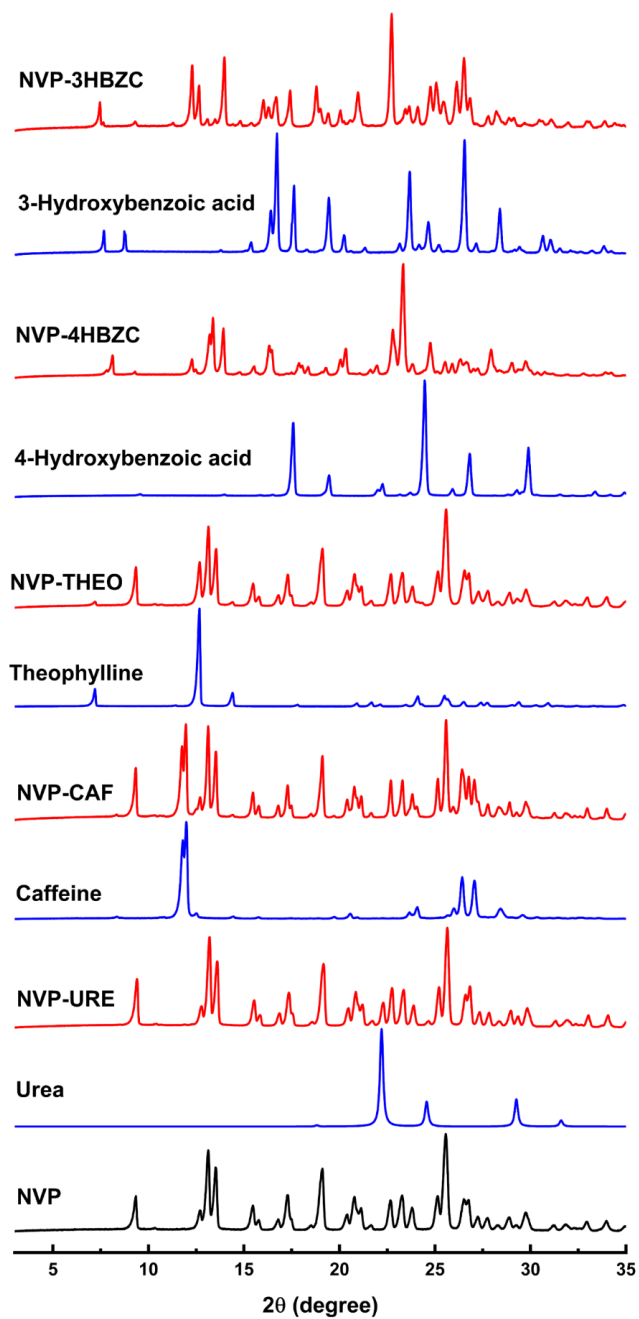


Figure S1. PXRD for NVP-3HBZC, NVP-4HBZC, NVP-THEO, NVP-CAF, and NVP-URE (red solid lines), for the pure co-former compounds (blue solid lines) and pure NVP compound (black solid lines).

Figure S2 exhibits the PXRD results for all NVP-SA samples compared to pure compounds and the structure reported by Caira and co-workers (CSD refcode: LATQUU).<sup>1</sup> Although the NVP-SA cocrystal was obtained, some differences were observed with respect to the reported structure. Figure S3 exhibits the PXRD results for all NVP-SAC samples compared to pure compounds and the structure reported by Caira and co-workers (CSD refcode: LATQOO).<sup>1</sup> In this case, we have obtained the same structure reported in the literature.

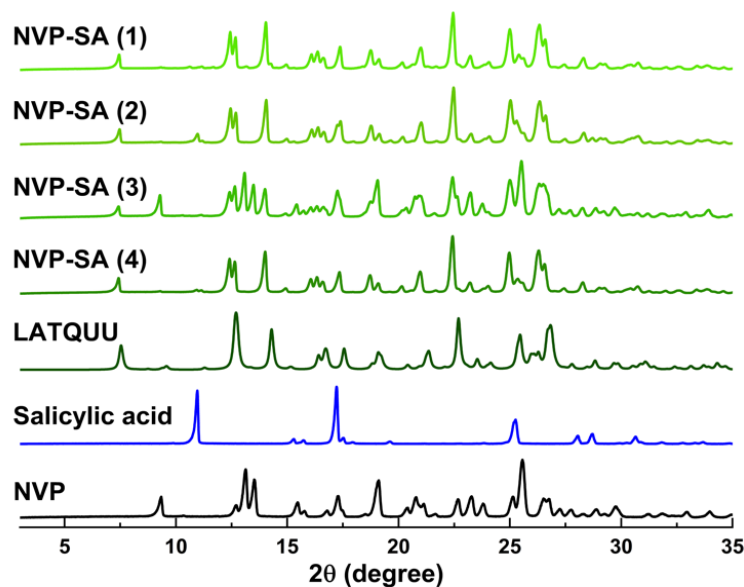


Figure S2. PXRD for NVP-SA samples (1), (2), (3) and (4) in comparison to the precursor materials NVP and SA and the reported structure of NVP-Salicylic acid

cocrystal (LATQUU).<sup>1</sup> Diffraction patterns (1) and (2) corresponding, respectively, to 1:1 and 2:1 stoichiometries prepared in methanol, whereas (3) and (4) corresponding, respectively, to 1:1 and 2:1 stoichiometries prepared in chloroform. Differences are observed at approximately 12.5° and in the region between 15° and 20°

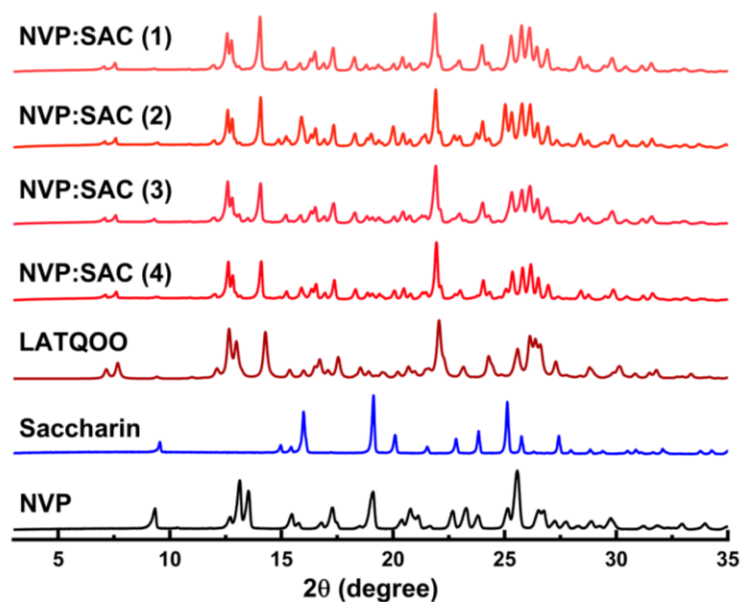


Figure S3. PXRD for NVP-SAC samples (1), (2), (3), and (4) in comparison with precursor materials NVP and Saccharin and reported structure for NVP-Saccharin co-crystal (LATQOO).<sup>1</sup> Diffraction patterns (1) and (2) corresponding, respectively,

to 1:1 and 2:1 stoichiometries prepared in methanol, whereas (3) and (4)

corresponding, respectively, to 1:1 and 2:1 stoichiometries prepared in chloroform.

*Solid-state NMR results:*

Solid-state NMR analysis was carried out in NVP-SA, NVP-SAC, NVP-THEO, NVP-CAF, and NVP-URE samples. Table S3 exhibits chemical shifts for NVP-SA co-crystals, pure NVP, and pure SA. Spectra for the other samples are shown in Figure S4.

Table S3. Chemical Shift for NVP, SA and NVP-SA cocrystal

C	NVP $\delta^{13}\text{C}$ [ppm]	SA $\delta^{13}\text{C}$ [ppm]	NVP-SA $\delta^{13}\text{C}$ [ppm]
1	170.3		170.3
2	122.7		123.8
3	154.2		154.1
4	161.8		164.5
5	121.7		120.1
6	140.6		138.1
7	119.2		116.8
8	152.6		152.4
9	143.7		142.6
10	121.0		120.1
11	141.3		142.6
12	18.4		18.9
13	29.7		31.3
14	11.04		12.01
15	11.04		12.01
16		111.9	112.8
17		133.0	131.7
18		121.1	116.8
19		138.5	139.8
20		118.2	119.3
21		162.1	162.2
22		176.1	172.3

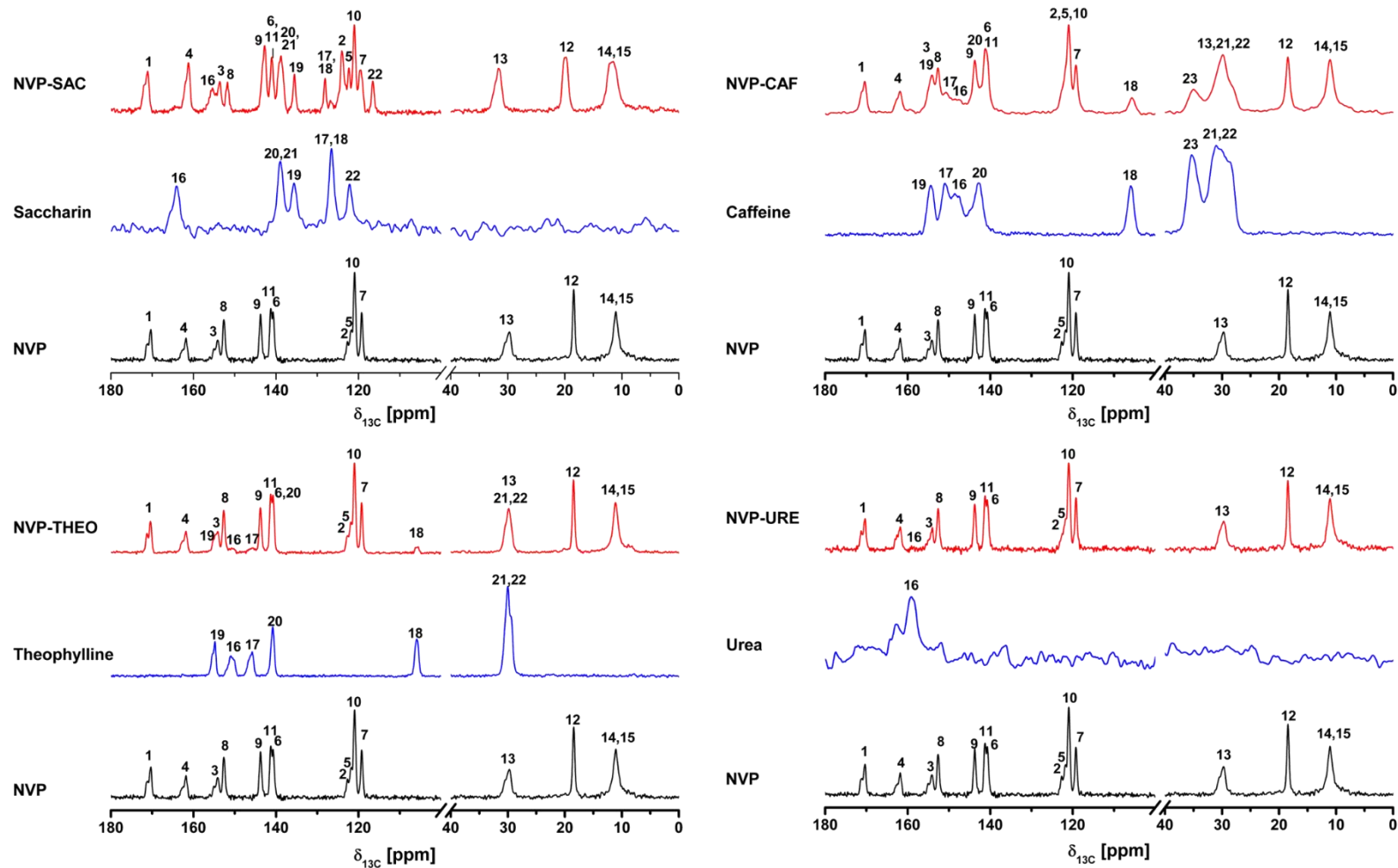


Figure S4. ssNMR spectra for NVP-SAC, NVP-THEO, NVP-CAF, and NVP-URE and its precursor materials.

*DSC results:*

Figure S5 exhibits the DSC curves obtained for the pure compounds and NVP-SA, NVP-SAC, NVP-3HBZC, NVP-4HBZC, NVP-THEO, NVP-CAF, and NVP-URE samples.

The NVP-SA sample showed three events, which have occurred at approximately 129.4 °C, 204.6 °C, and 249.0 °C. SA presents a thermal event around 162.8 °C and agrees with the melting point for SA described in the literature. The degradation process of SA starts at approximately 210 °C. Although the peak at 249.0 °C corresponds to the NVP melting point, which occurs at 247.8 °C, this peak cannot indicate NVP excess. The herein recorded thermal behavior can be explained by the fact that the cocrystal melts at 204.6 °C. Since SA melts at 162.8 °C and this process is followed by degradation when the cocrystal melts under higher temperatures, the SA (now free) degrades and remains as NVP crystals that melt lately.

The DSC curve for NVP-SAC cocrystal presented an event occurring at proximately 214.6 °C, which corresponds to the melting point of this structure,



followed by a decomposition event at 224.3 °C. Since the NVP presents a melting point at 247.8 °C and SAC decomposes at 227.3 °C, these thermal profiles can be interpreted as a cocrystal formation indicative. The decomposition event in NVP-SAC is due to the degradation of SAC, which was in a free form after the melting of the cocrystal.

The DSC curve for NVP-4HBZC exhibits a unique event at 214.3 °C, corresponding to the melt of the phase, followed by the degradation process from 270.9 °C. Although the temperature of melting is close to the melt of pure 4HBZC, which occurs at 217.8 °C, there is no event related to the melting of pure NVP.

The DSC curve for NVP-3HBZC exhibits two events. The first event occurs around 173.0 °C and it is not corresponding to any event in the pure compounds. The second event occurs around 203.8 °C and corresponds to the melt of 3HBZC. These results corroborate PXRD results and also indicates the presence of a new cocrystal and an excess of 3HBZC, indicating that the cocrystal exhibits a stoichiometry different from 1:1.

The DSC analysis for NVP-URE shows an event occurring at approximately 126.1 °C, which corresponds to the melting point of URE at 135.5 °C. Besides, there is a second event starting at approximately 200.0 °C, with a maximum peak at 237.5 °C. This second event corresponds to an overlap of two events: the URE degradation that starts approximately at 180 °C, and NVP melting fusion that occurs at 247.8 °C. This agrees with PXRD and ssNMR results, allowing to conclude that NVP-URE is definitely a physical mixture of pure crystalline phases.

The curves obtained for NVP-THEO exhibits two melting points at 223.6 °C and 234.1 °C. These points do not correspond to melting points obtained for pure NVP and pure THEO, which are in 247.8 °C and 274.7 °C, respectively. The same behavior is observed for NVP-CAF. Pure CAF exhibits two events, at 155.8 °C and 238.6 °C. According to the literature, the first event is related to the phase transition in CAF.<sup>2</sup> The DSC curve for the NVP-CAF exhibits three events at 163.1 °C, 204.4 °C, and 212.8 °C. The event at 163.1 °C is also related to the phase transition in CAF. However, the following two events do not correspond to pure CAF or pure NVP. Correlation with PXRD results, allow concluding that NVP-

THEO and NVP-CAF are eutectic systems. Figure S6 exhibits the curves obtained for NVP-THEO and NVP-CAF at different composition ratios.

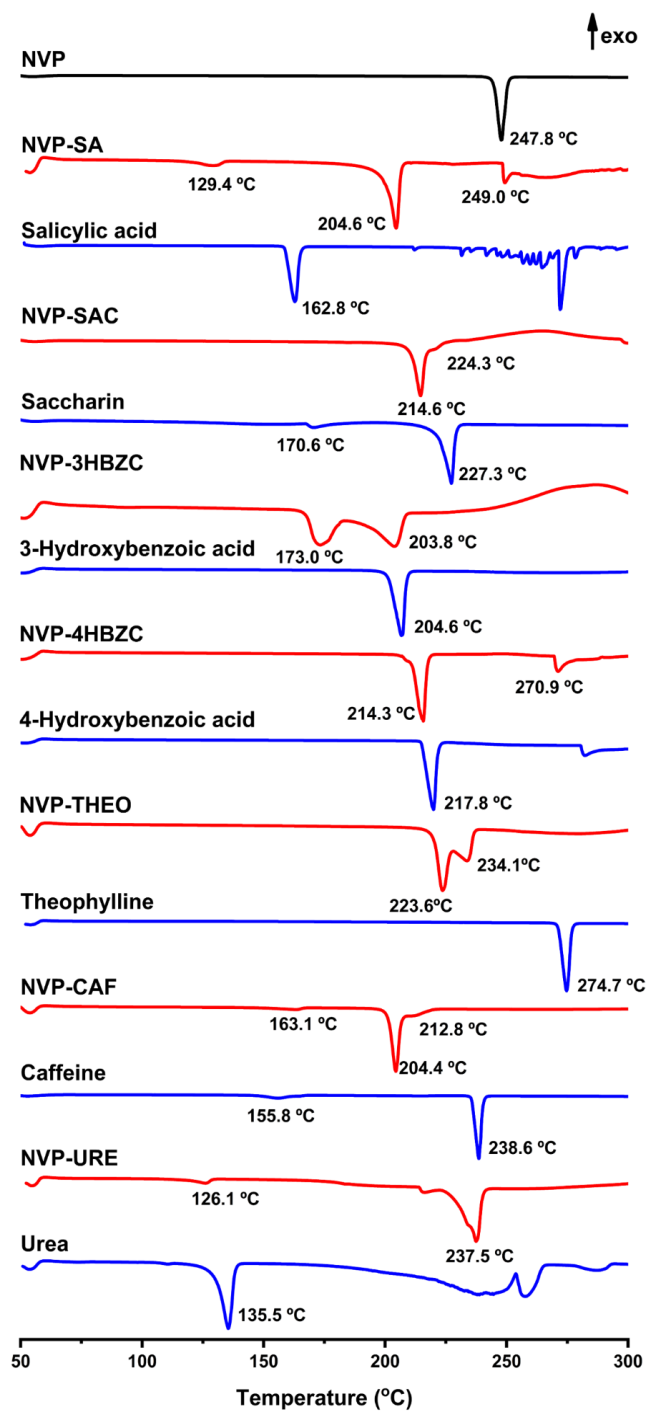


Figure S5. DSC curves for NVP-SA, NVP-SAC, NVP-3HBZC, NVP-4HBZC, NVP-THEO, NVP-CAF, and NVP-URE in comparison with pure compounds.

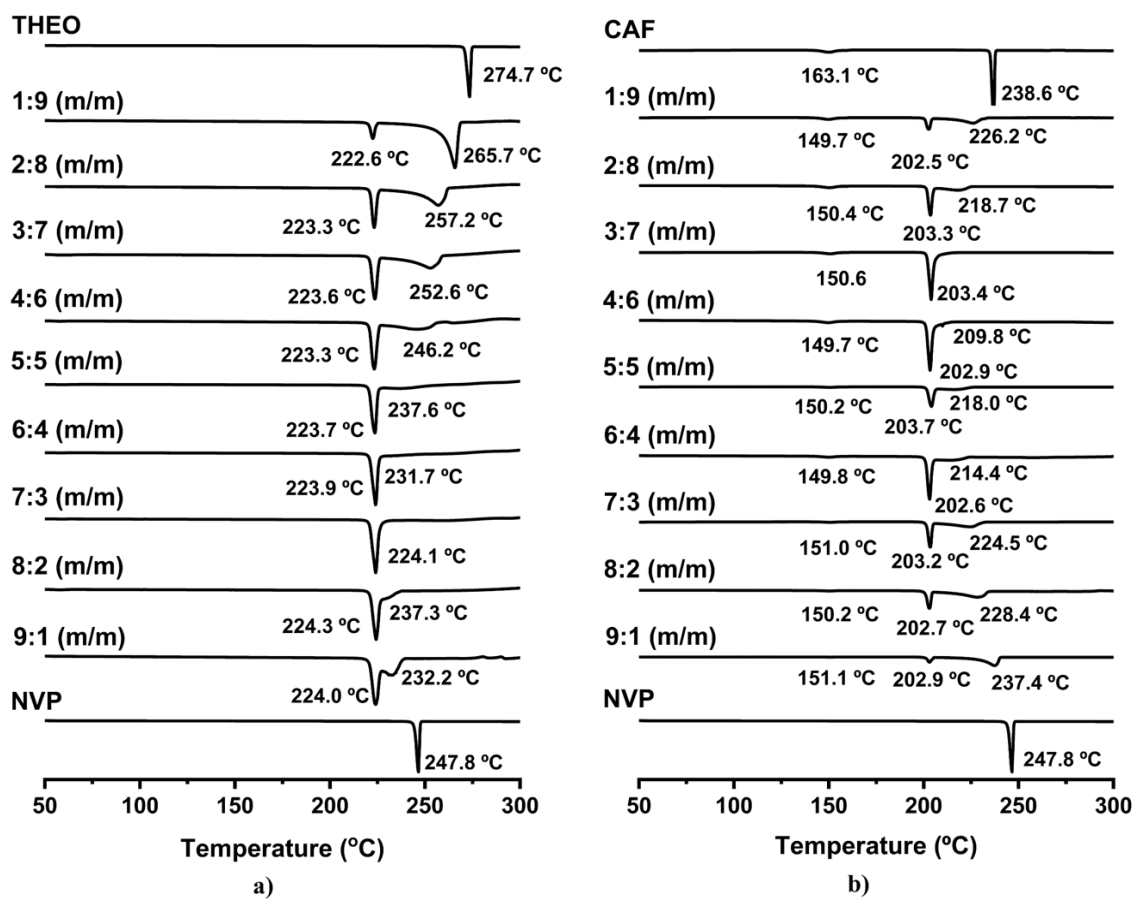


Figure S6. DSC curves for a) NVP-THEO and b) NVP-CAF, at different ratios.

Table S4. Crystallographic data for NVP-SA at room temperature and 100 K, and NVP-4HBZC.

Empirical formula	$2(\text{C}_{15}\text{H}_{14}\text{N}_4\text{O}) \cdot (\text{C}_7\text{H}_6\text{O}_3)$	$2(\text{C}_{15}\text{H}_{14}\text{N}_4\text{O}) \cdot (\text{C}_7\text{H}_6\text{O}_3)$	$(\text{C}_{15}\text{H}_{14}\text{N}_4\text{O}) \cdot (\text{C}_7\text{H}_6\text{O}_3)$
Formula weight	670.72	670.72	404.42
Temperature/K	290	100	300
Crystal system	Triclinic	Triclinic	Monoclinic
Space group	P-1	P-1	C2/c
a/Å	7.1767(4)	11.1691(11)	24.318(5)
b/Å	9.6278(5)	12.5867(13)	7.5618(13)
c/Å	11.9235(6)	13.3946(14)	23.242(5)
$\alpha/^\circ$	96.865(2)	113.295(3)	90
$\beta/^\circ$	93.039(2)	99.352(3)	111.321(8)
$\gamma/^\circ$	98.126(2)	107.282(3)	90
Volume/Å <sup>3</sup>	807.69(7)	1565.0(3)	3981.3(14)
Z	1	2	1
$\rho_{\text{calc}}/\text{g/cm}^3$	1.379	1.423	1.349
$\mu/\text{mm}^{-1}$	0.095	0.098	0.783
F (000)	352.0	704.0	1696.0
Crystal size/mm <sup>3</sup>	0.312 × 0.219 × 0.126	0.312 × 0.219 × 0.126	0.12 × 0.12 × 0.10
Radiation	MoK $\alpha$ ( $\lambda$ = 0.71073)	MoK $\alpha$ ( $\lambda$ = 0.71073)	CuK $\alpha$ ( $\lambda$ = 1.54178)
2 $\theta$ range of data collection/ $^\circ$	6.902 to 51.354	4.32 to 50.692	

Index ranges	-8 ≤ h ≤ 8, -11 ≤ k ≤ 11, -14 ≤ l ≤ 14	-13 ≤ h ≤ 13, -15 ≤ k ≤ 15, -16 ≤ l ≤ 16	-28 ≤ h ≤ 28, -9 ≤ k ≤ 8, -26 ≤ l ≤ 27
Collected reflections	24244	46332	17411
Independent reflections	3059 [R <sub>int</sub> = 0.0407, R <sub>sigma</sub> = 0.0205]	5725 [R <sub>int</sub> = 0.1138, R <sub>sigma</sub> = 0.0484]	[R <sub>int</sub> = 0.1414, R <sub>sigma</sub> = 0.0822]
Data/restraints/parameters	3059/69/260	5725/0/455	3556/0/275
Goodness-of-fit on F <sup>2</sup>	1.068	1.014	1.034
Final R indices [I ≥ 2σ (I)]	R <sub>1</sub> = 0.0428, wR <sub>2</sub> = 0.1052	R <sub>1</sub> = 0.0501, wR <sub>2</sub> = 0.1122	R <sub>1</sub> = 0.0683, wR <sub>2</sub> = 0.1487
Final R indices [all data]	R <sub>1</sub> = 0.0602, wR <sub>2</sub> = 0.1204	R <sub>1</sub> = 0.0954, wR <sub>2</sub> = 0.1335	R <sub>1</sub> = 0.1449, wR <sub>2</sub> = 0.1859
Largest diff. peak/hole/eÅ <sup>-3</sup>	0.16/-0.16	0.66/-0.24	0.25/-0.21

---

Table S5. Relationship between the centers of inversion in the NVP-SA cocrystal structures solved at room temperature and 100K.

Wyckoff letter in the structure at room temperature	Coordinates at RT	Coordinates at 100K
1a	0, 0, 0	0, ½, 0
1b	0, 0, ½	-
1c	0, ½, 0	-
1d	½, 0, 0	-
1e	½, ½, 0	½, ½, 0
1f	½, 0, ½	½, 0, ½
1g	0, ½, ½	½, ½, ½
1h	½, ½, ½	-

**T** is the transformation matrix from the RT unit cell to the LT unit cell.

$$T = \begin{pmatrix} 1 & 1 & 0 \\ 1 & -1 & 0 \\ 0 & 1 & -1 \end{pmatrix}$$



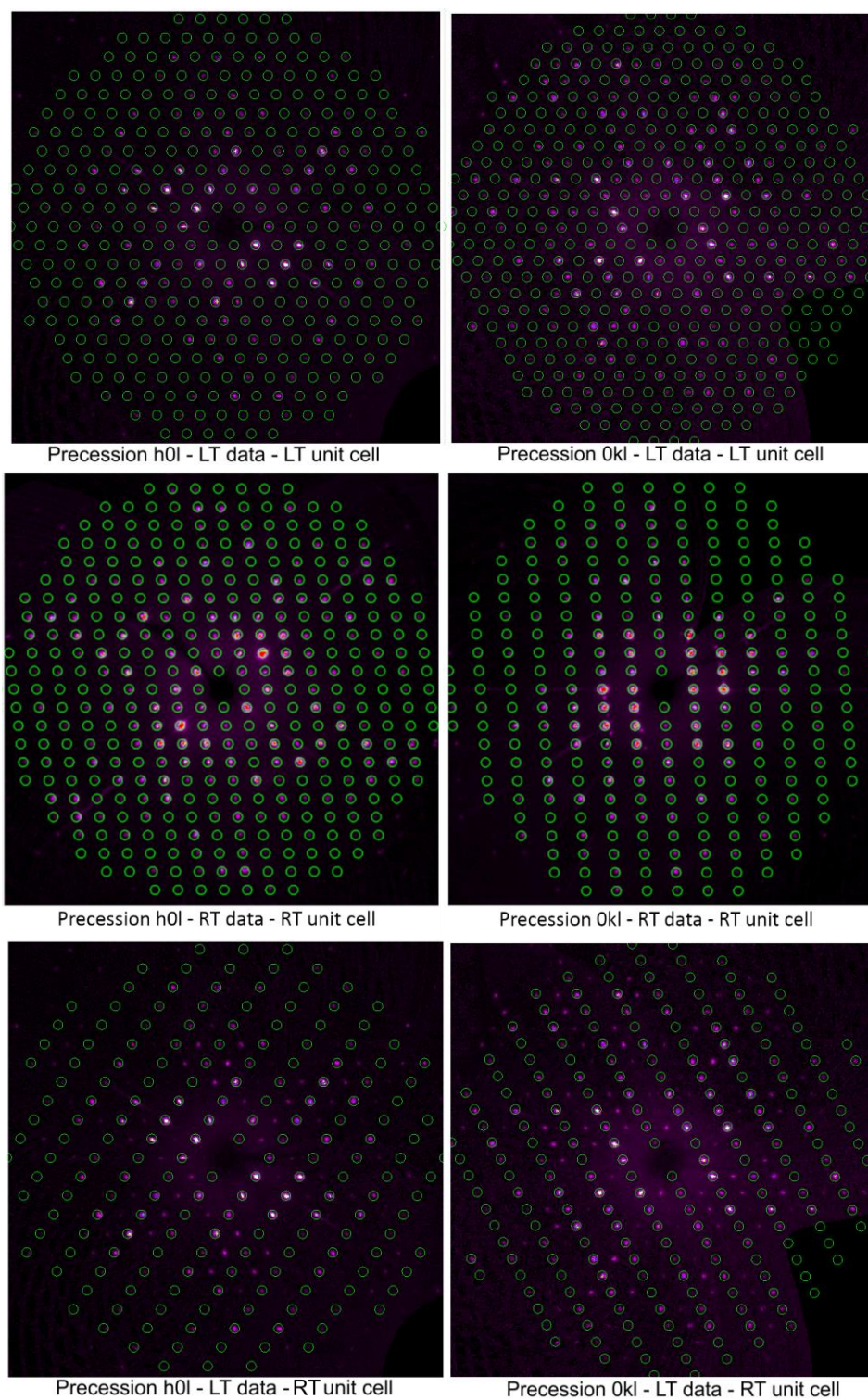


Figure S7. Precession image results for NVP-SA crystal at low temperature (LT) and room temperature (RT).

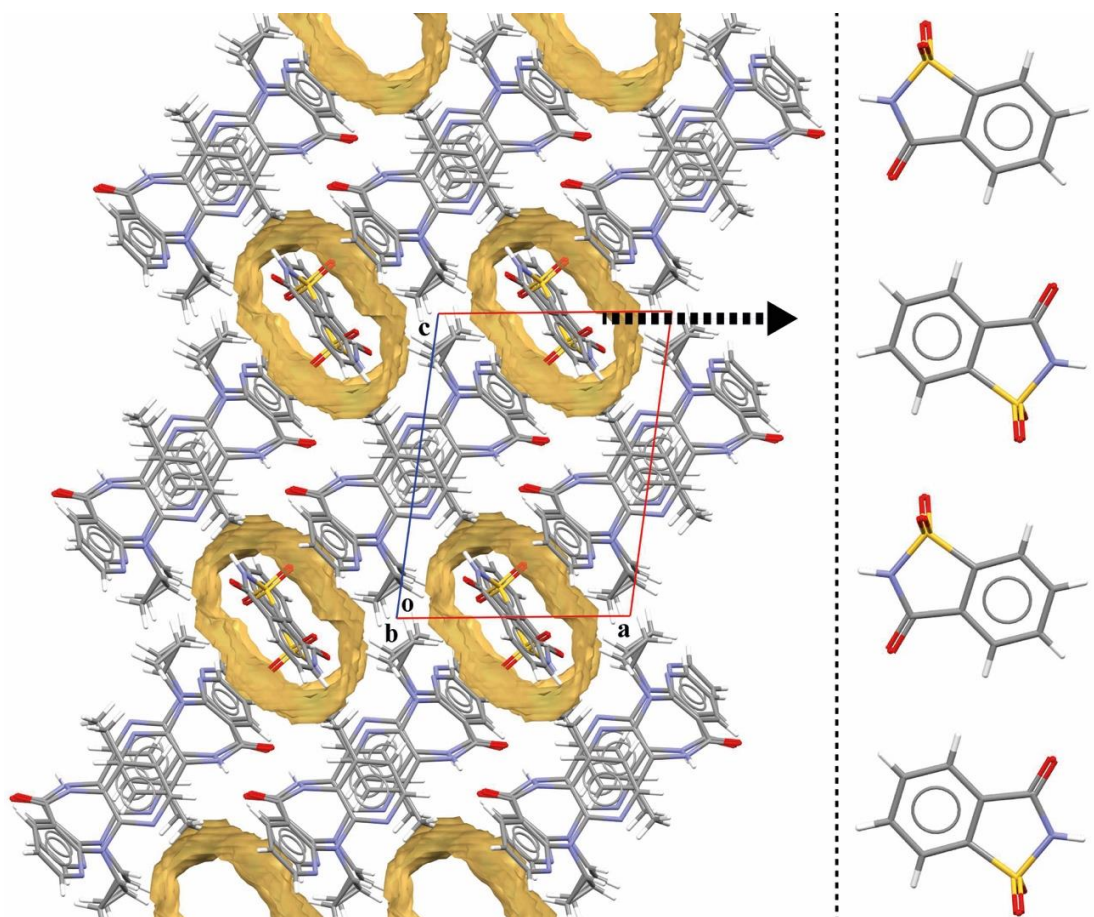


Figure S8. Structure of LATQOO showing the pipe-shaped voids in yellow and on the right, the extended projection of the observed SAC tapes that fit in those channels.

the SPXRD experiment was conducted in order to assess the structural behavior from different temperatures and to confirm the models of the crystalline structure at room and low temperature. Figure S9 shows the comparison of diffraction patterns between

calculated and experimental data. These comparisons show the agreement between our crystalline structure determination and SPXRD results. However, some differences could be seen between Caira's calculated pattern at low temperature, according to the observation in Figure S9.

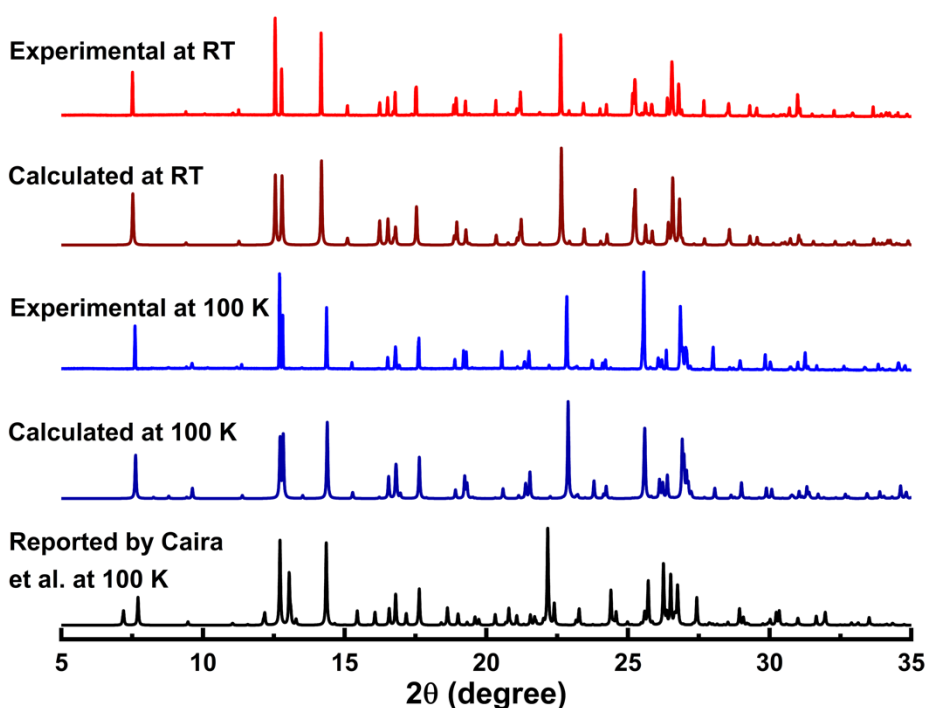


Figure S9. Diffraction patterns obtained for NVP-SA (1) from experimental SPXRD and calculated from the SXR data, at room and 100 K temperatures for both, and the calculated from the structure reported by Caira and co-workers for comparison porpoise.

Reference:

- (1) Caira, M. R.; Bourne, S. A.; Samsodien, H.; Engel, E.; Liebenberg, W.; Stieger, N.; Aucamp, M. Co-Crystals of the Antiretroviral Nevirapine: Crystal Structures, Thermal Analysis and Dissolution Behaviour. *CrystEngComm* **2012**, *14* (7), 2541–2551.
- (2) Murugan, N. A.; Sayeed, A. Thermal Behavior of Disordered Phase of Caffeine Molecular Crystal: Insights from Monte Carlo Simulation Studies. *J. Chem. Phys.* **2009**, *130* (20), 204514.